# A Global ab Initio Potential Energy Surface for Formaldehyde†

**Xiubin Zhang,‡ Shengli Zou,‡,§ Lawrence B. Harding,|| and Joel M. Bowman*,‡**

*Department of Chemistry and Cherry L. Emerson Center for Scientific Computation, Emory University, Atlanta, Georgia 30322, and Chemistry Division, Argonne National Laboratory, Argonne, Illinois 60439*

*Received: April 15, 2004; In Final Form: May 17, 2004*

We report a global potential energy surface for formaldehyde. The surface is a combination of six local fits joined smoothly by five switching functions. The fits are to roughly 80000 CCSD(T)/aug-cc-PVTZ and 53000 MR−CI/aug-cc-PVTZ calculations of electronic energies. The surface describes the $H_2CO$ minimum, the cis and trans HCOH isomers, the molecular channel, $H_2$+CO, and the radical channel, H+HCO. The properties of the potential are evaluated by analyzing the properties of the six stationary points, one-dimensional cuts, and contour plots of the fit.

## I. Introduction

The photochemistry of formaldehyde has been extensively explored both experimentally[1−9] and theoretically[10−20] since the 1970s. This intense interest is due to the importance of formaldehyde in atmospheric, interstellar, and combustion chemistry. The mechanism of its photodissociation is reasonably well known[3] to be due to fluorescence or internal conversion from the electronically excited $H_2CO$ ($S_1$) to the ground-state $H_2CO$ ($S_0$) with a high degree of vibrational excitation. (The details of this internal conversion are not presently known, however.) The ground-state complex then may dissociate to two sets of products: $H_2$+CO or H+HCO. An alternative path to H+HCO is by $S_1$ intercrossing to $T_1$ and the subsequent dissociation.[6−8] Moore has also suggested the existence of a second mechanism to form the molecular products via the exit radical channel reaction H+HCO → $H_2$+CO.[9] Thus, to fully address the dynamics of this unimolecular reaction theoretically a potential surface that is fully global is necessary.

Several previous theoretical studies have focused on the properties of stationary points[10−16] and the classical molecular dynamics[17,18,21,22] related to the molecular products channel ($H_2$-CO→$H_2$+CO). The corresponding saddle point is well characterized, and the best calculations predict a barrier 2−3 kcal/mol higher than the experimental estimate.[16] Several semiglobal potential energy surfaces (PES) have been designed for dynamics studies[19−23] of the molecular channel. In 1981, Handy and Carter[23] reported an empirical surface with a many-body expansion formula. This surface can also be used to study any possible fragmentation reaction of formaldehyde, for example, radical dissociation into H+HCO or molecular dissociation into $H_2$+CO. However, a classical trajectory calculation[4] using this surface did not reproduce the experimental distributions well. Miller and co-workers[22] constructed two global potential energy surfaces for the $H_2CO$ → $H_2$+CO reaction by fitting to MP2/DZP and CCSD/TZ2P energies using the empirical valence-bond (EVB) approach. Trajectory calculations using one of these (CCSD PES) give good agreement with experimental data for the product-state distributions of $H_2$ and CO. Very recently, to study the role of isomerization in the molecular dissociation process by classical trajectory calculations, Yonehara and Kato[21] developed a PES by employing a modified Shepard interpolation method.[24] This surface can describe both the molecular dissociation and isomerization channels in a consistent way; however, it does not describe the radical channel H+HCO.

Our goal is to obtain a global potential surface that contains the isomers of $H_2CO$ as well as the molecular and radical dissociation channels and to use this surface in a variety of dynamics studies of formaldehyde dissociation. Furthermore, we are also interested in modeling the second abstraction reaction[9] H+HCO → $H_2$+CO, which connects the radical channel with the molecular one. To perform these complete dynamics studies, we need an accurate global PES that covers all of the regions of interest, that is, cis and trans HCOH, $H_2CO$, $H_2$+CO, and H+HCO.

In the present work, we develop such a global potential energy surface on the basis of two sets of high level (CCSD(T)/aug-cc-PVTZ and MR−CI/aug-cc-PVTZ) ab initio calculations. The paper is organized as follows. In the next section, we describe the details of the ab initio calculations and fitting procedures. The properties of the fitted potential energy surface are evaluated in Section III. We close with a summary and comments on future work in Section IV.

## II. Ab Initio Calculations and Fitting Procedures

A significant problem in fitting global surfaces is the choice of electronic wave functions. Finding a balance between cost and range of applicability is usually difficult. In the present case, this problem can be seen by noting that some regions of this potential surface, $H_2CO$, HCOH, and $H_2$+CO and reaction paths connecting these minima, can be well described with efficient, accurate, single-reference methods, such as CCSD(T), while other regions, H+HCO and H+H+CO, are inherently multi-reference in character and cannot be well characterized with any of the currently available single reference methods. The approach we have taken here to obtain a global surface is to first divide the potential into six overlapping local regions. Those local regions where single reference methods are expected to work well were characterized with CCSD(T) calculations. Local

† Part of the "Gert D. Billing Memorial Issue".

* Corresponding author. Fax: 1-404-7276628; e-mail address: bowman@euch4e.chem.emory.edu.

‡ Emory University.

§ Current address: Department of Chemistry, Northwestern University, 2145 Sheridan Road, Evanston, IL 60208-3113.

|| Argonne National Laboratory.

10.1021/jp048339l CCC: $27.50 
Published on Web 06/25/2004

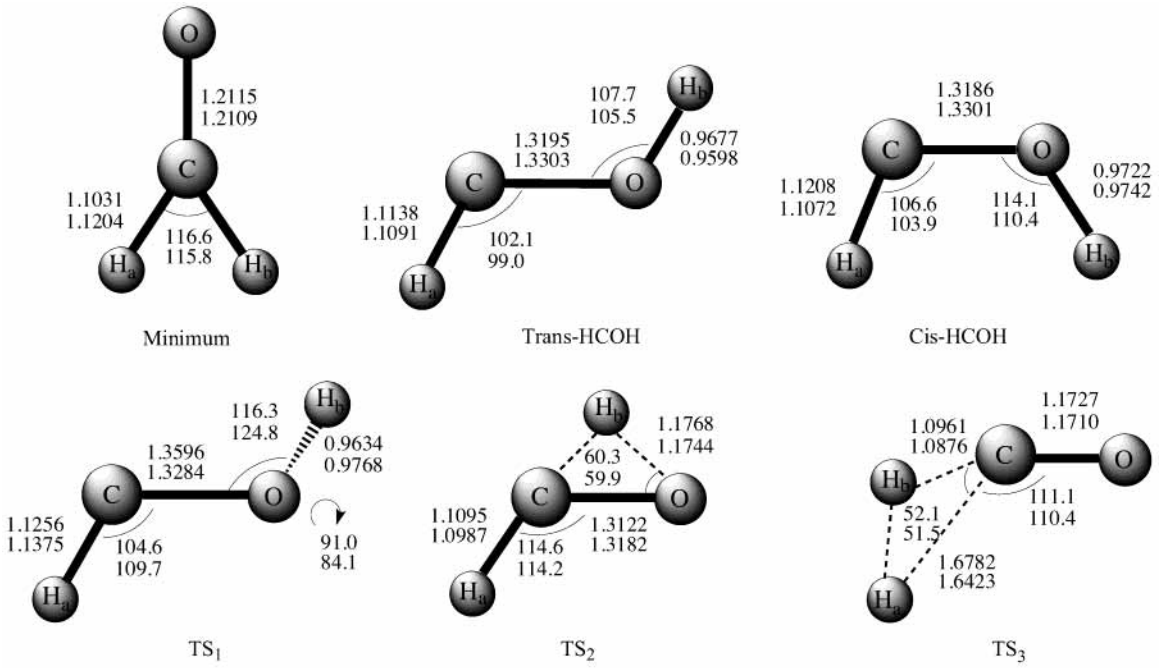


**Figure 1.** Optimized geometries of minima and saddle points on the fit (lower) and the corresponding ab initio values (upper). Bond distance is in angstrom and angle in degree.

regions where single reference methods are expected to perform poorly were characterized with a multireference configuration interaction (MR−CI) approach. A small shift in the energies of all of the MR−CI calculations was done in the region of overlap to make the absolute energy from that method agree with the one from CCSD(T) calculations. Then, local fits were made using an iterative procedure, where many ab initio points were generated and then fit. On the basis of the properties of the fit, more ab initio points were added to the data set and then refit. This continued until a satisfactory local fit was obtained. Then, the local fits were smoothly joined by switching functions. Additional ab initio calculations were done in the interfacial regions of the switching and used in refitting to obtain a final satisfactorily smooth result. The details of these procedures are given below.

**A. Coordinate Systems.** In this section, we define the coordinates used in generating and fitting the ab initio points and in the switching functions connecting the local fits. All fitting was done using the six internuclear distances, $R_{CHa}$, $R_{CHb}$, $R_{CO}$, $R_{OHa}$, $R_{OHb}$, and $R_{HH}$, sometimes denoted below as $r_1-r_6$, respectively. For some switching functions, we define reduced internucluear distances as follows:

$$S_{CHa} = R_{CHa}/R_0(CH) \tag{1}$$

$$S_{CHb} = R_{CHb}/R_0(CH) \tag{2}$$

$$S_{OHa} = R_{OHa}/R_0(OH) \tag{3}$$

$$S_{OHb} = R_{OHb}/R_0(OH) \tag{4}$$

$$S_{HH} = R_{HH}/R_0(HH) \tag{5}$$

where $R_0(CH) = 2.15$, $R_0(OH) = 1.85$, and $R_0(HH) = 1.45$ bohr. (Hereafter, distances are always in bohr, with the exception of Figure 1 where they are in angstrom.)

While the internuclear distances are convenient for fitting, they are not particularly convenient for generating input for all of the ab initio calculations. Thus, two additional sets of coordinates were also used. One set is the six Jacobi coordinates $R_{HH}$, $R_{CO}$, $R$, $\theta_1$, $\theta_1$, and $\varphi$, where $R$ is the distance between the centers of masses of HH and CO, $\theta_1$ the angle between the vectors $\mathbf{R}_{HH}$ and $\mathbf{R}$, $\theta_2$ is the angle between the vectors $\mathbf{R}_{CO}$ and $\mathbf{R}$, and $\varphi$ is the out-of-plane torsion angle. The other set of coordinates, which we denote set II, consists of $R_{CO}$, $R_{MHa}$, $R_{MHb}$, $\alpha_a$, $\alpha_b$, and $\beta$, where $R_{MHa}$ is the distance from $H_a$ to the center of mass of the CO fragment (M), $R_{MHb}$ is the M−$H_b$ distance, $\alpha_a$ is the $H_a$−M−C angle, $\alpha_b$ is the $H_b$−M−C angle, and $\beta$ is the dihedral angle between the $H_aCO$ and $H_bCO$ planes.

**B. Switching Functions.** In this section, we define the switching functions used to connect the six local fits. The switching functions are designed to switch smoothly from 1.0 to 0.0 in the range $S_{min} \le S \le S_{max}$. To do this, we first define $X$ as follows:

$$X = (S - S_{min})/(S_{max} - S_{min}) \tag{6}$$

then the switching function, $W$, is

$$W = 1.0 - 10X^2 + 15X^4 - 6X^5 \tag{7}$$

This is a monotonic function in the interval $S_{min} \le S \le S_{max}$; it is 1.0 at $S_{min}$, 0.0 at $S_{max}$, and its first and second derivatives are zero at the two end points. With different choices for $S$, $S_{min}$, and $S_{max}$, this function is used to switch between all six local fits.

To switch between the CCSD(T) fits and the MR−CI fits $S$, $S_{min}$, and $S_{max}$ are defined such that $S < S_{max}$ corresponds to regions where the CCSD(T) wave function is expected to behave well. This is accomplished by first defining switching coordinates for hydrogen atoms a and b as follows:

$$S_a = \min(S_{CHa}, S_{OHa}, S_{HH}) \tag{8}$$

$$S_b = \min(S_{CHb}, S_{OHb}, S_{HH}) \tag{9}$$

Finally the combined switching coordinate is defined as

$$S = \max(S_a, S_b) \tag{10}$$

This switching coordinate is a measure of the distance of the furthest hydrogen atom from its nearest neighbor. By design, the switching coordinate, $S$, is large in regions of the potential surface where the electronic wave function is expected to have a lot of biradical character (near the H+HCO and H+H+CO asymptotes). For the switch from the CCSD(T) potential to the MR−CI potential, we set $S_{min} = 1.5$ and $S_{max}=2.0$. In this way, whenever one of the hydrogens is more than twice $R_0$ from its nearest neighbor the CCSD(T) fit is switched off.

**C. Ab initio Calculations.** The electronic structure calculations were done using the MOLPRO package of codes[25] and employ the Dunning augmented correlation consistent polarized valence triple-$\zeta$ basis set.[26−28] The CCSD(T) calculations employ the closed shell, spin restricted, coupled cluster theory (restricted to single and double excitations with perturbative triple excitations) of Hampel et al.[29]

The MR−CI calculations employ the internally contracted, singles and doubles CI formalism of Werner et al.[30,31] The orbitals for the CI calculations are optimized using the complete active space, self-consistent field (CASSCF) methodology. In these calculations, the CASSCF reference wave function consists of six active orbitals and six active electrons. The six active orbitals include two CH $\sigma$ orbitals, two CH $\sigma$* orbitals, the CO $\pi$ orbital, and the CO $\pi$* orbital. The effects of higher order excitations were approximated using a multireference Davdison correction.

**D. CCSD(T) Fits.** On the basis of the CCSD(T) calculations, three separate fits, denoted i, ii, and iii, were done. In fit i, several sets of grids were used. First, a fine grid (bond displacements of 0.005 A) of roughly 300 points was sampled about each stationary point (three minima and three saddle points shown in Figure 1). An additional 15 000 points were randomly sampled around and between these six stationary points, using fairly large displacements, but not so large as to sample very high energy regions. These points were augmented by approximately 50 000 points in six Jacobi coordinates. The ranges for these variables are $1 \le R_{HH} \le 9$, $1 \le R_{CO} \le 4$, $0 < R \le 6$, $-1 \le \cos(\theta_1) \le 1$, $-1 \le \cos(\theta_2) \le 1$, and $0 \le \varphi \le \pi$. All together, we obtained a total of about 80 000 electronic energies. These calculations were done on "Multinode", which is our 42-node cluster of Dual XEON 2.4GHz processors.

A total of 15 668 ab initio energies, which expands to 31 336, using permutation symmetry with respect to the two H atoms, with energies below 38 500 cm$^{-1}$ were used in the fit. The fitting procedure employed in the present study is similar to the one used previously for fitting the $C_2H_2$ potential.[32] The functional form of the potential is a direct product, multinomial in Morse variables for six internuclear distances $r_i$, $i = 1-6$:

$$V(r_1...r_6) = \sum_{n_1,n_2...n_6} C_{n_1...n_6} \prod_{i=1}^{6} (1 - e^{-\alpha(r_i - r_{ie})})^{n_i} \qquad (11)$$

where the set of integers $n_1-n_6$, is restricted as follows: $n_3$ is less than or equal to 3 and the sum $n_1 + n_2...+ n_6$ is less than or equal to 6. With these restrictions, expression 11 contains a total of 896 terms. Also, $\alpha$ is set to 0.5 in the fit and $r_{ie}$ $i = 1-6$ are the equilibrium geometry values of the molecule at the global minima of formaldehyde, ($r_{1e}$ and $r_{5e}$ equal 3.8215, $r_{2e}$ and $r_{4e}$ equal 2.0845, $r_{3e}$ and $r_{6e}$ equal 2.2895 and 3.5467, respectively). The accuracy of the fit was determined by calculating the RMS error as a function of maximum energy as shown in Table 1.

This fit looks reasonable out to $R$ of about 5, which is well beyond the $H_2$+CO saddle point. To correctly describe the asymptotic behavior of the molecular channel, another fit, ii, was generated using new data over the following grid in the six Jacobi coordinates:

$R_{HH} = 1.0, 1.2, 1.4, 1.6, 1.8, 2.1, 2.5, 2.8, 3.0, 3.5, 4.0$

$R_{CO} = 1.9, 2.0, 2.1, 2.2, 2.3, 2.4, 2.5, 2.8, 3.5$

$R = 3.5, 4.0, 4.5, 5.5, 6.0, 6.5, 8.5, 9.5, 10.5, 11.0$

$\theta_1 = 9.7, 43.6, 83.1$ deg

$\theta_2 = 9.7, 43.6, 83.1, 131.8, 172.0$ deg

$\varphi = 9.7, 43.6, 83.1$ deg From the total of 44 550 points, 9523 (19046 permutation symmetry equivalent) points with maximum energy less than 38 500 cm$^{-1}$ were used for the fitting. The corresponding analytical function is a polynomial in Morse variables including 868 terms (third order in CO and HH bond lengths, sixth order in other internuclear distances). The RMS of this fit is 174.7 cm$^{-1}$.

**TABLE 1: The RMS Fitting Error of the CCSD(T) Fit (i) (Defined in the Text) as a Function of Energy, $E$[a]**

| $E$ (cm$^{-1}$) | RMS (cm$^{-1}$) | sample points |
|---|---|---|
| 38 500 | 648 | 31 336 |
| 35 000 | 556 | 26 972 |
| 30 000 | 482 | 18 916 |
| 25 000 | 437 | 11 896 |
| 20 000 | 408 | 7368 |
| 15 000 | 405 | 4322 |
| 10 000 | 277 | 2878 |

[a] The number of ab initio (sample) points in the given energy range is also given.

At large $R$, that is, in the $H_2$ + CO channel, the potential should only depend on $R_{HH}$ and $R_{CO}$. At $R = 8$, fit ii is nearly independent of the Jacob angles and at $R = 10$ it is essentially independent of these angles. To extend the potential beyond $R = 10$ we performed a simple final fit, iii. This was done using 30 electronic energies obtained by varying $R_{HH}$ from 1 to 3 and fixing $R_{CO} = 2.1486$, with $R = 9$, $\theta_1 = 90$ deg, $\theta_2 = 0$ deg, and $\varphi = 0$ deg. Another 30 electronic energies were generated by varying $R_{CO}$ from 1.5 to 3 and fixing $R_{HH} = 1.4263$, and the other coordinates were fixed at the same value above. Then, we did a simple one-dimensional fit of the $H_2$ potential and another one for CO by using the following functional forms:

$$V_{HH} = \sum_{n=0}^{3} C_n [1 - e^{-\alpha(r_{HH} - r_{HH,e})}]^n \qquad (12)$$

$$V_{CO} = \sum_{n=0}^{3} D_n (1 - e^{-\alpha(r_{CO} - r_{CO,e})})^n \qquad (13)$$

where $r_{HH,e} = 1.4263$ and $r_{CO,e} = 2.1486$ corresponding to minimum values from fit ii PES at the configuration where $R = 9$, $\theta_1 = 90$ deg, $\theta_2 = 0$ deg, and $\varphi = 0$ deg. The analytical representation of fit iii is finally

$$V_{HH+CO} = V_{HH} + V_{CO} + 1931.63 \text{ cm}^{-1} \qquad (14)$$

and 1931.63 cm$^{-1}$ is the energy of the PES for $H_2(r_{HH,e})$+CO($r_{CO,e}$) relative to the minimum of $H_2CO$.

To combine the three CCSD(T) fits, we chose $R$ as the switching coordinate. In the range of $4.5 < R < 5.5$, fit i switches to fit ii, and in $9.5 < R < 10.0$ fit ii switches to fit iii.

**E. MR−CI Fits.** MR−CI calculations were carried out at ~53 000 symmetry unique points using the set II coordinates defined above. Of these, approximately 7000 were discarded because they were more than 17 500 cm$^{-1}$ (50 kcal/mol) above the H+HCO asymptote. The remaining ~46 000 points cover the following ranges of coordinates: $1.7 < R_{CO} < 3.0$, $1.3 <$

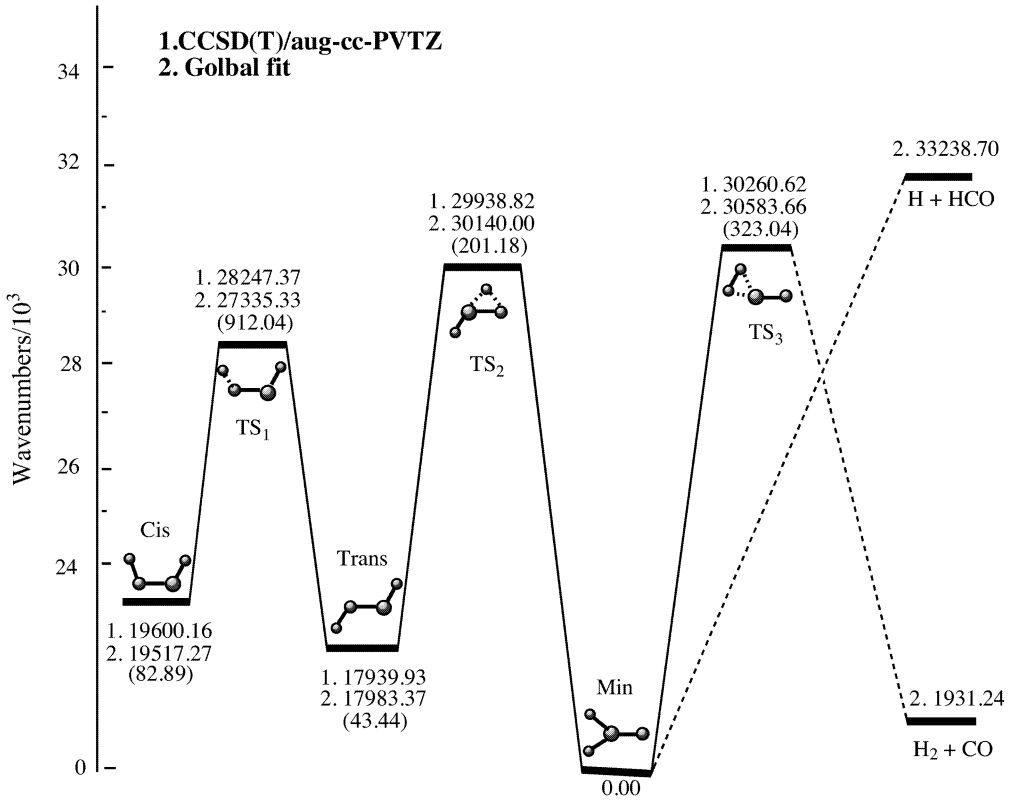


**Figure 2.** The ab initio (upper) and fitted (lower) relative energies of minima and saddle points in wavenumber. The values in parentheses are the differences.

**TABLE 2: The Harmonic Frequencies ($cm^{-1}$) of Minima and Saddle Points on the CCSD(T) Fit Are Compared with Those from ab Initio Calculations**[a]

| stationary point | | $\omega_1$ | $\omega_2$ | $\omega_3$ | $\omega_4$ | $\omega_5$ | $\omega_6$ |
|---|---|---|---|---|---|---|---|
| min | PES | 1164 | 1337 | 1623 | 1806 | 2810 | 2949 |
| | ab initio | 1180 | 1258 | 1529 | 1764 | 2931 | 2997 |
| trans | PES | 1108 | 1281 | 1369 | 1714 | 2927 | 4098 |
| | ab initio | 1078 | 1210 | 1312 | 1505 | 2863 | 3737 |
| cis | PES | 1221 | 1342 | 1440 | 1608 | 2741 | 3839 |
| | ab initio | 999 | 1226 | 1313 | 1471 | 2772 | 3625 |
| $T_{s1}$ | PES | 1074i | 968 | 1208 | 1465 | 2541 | 3531 |
| | ab initio | 1483i | 751 | 1174 | 1400 | 2723 | 3857 |
| $T_{s2}$ | PES | 2068i | 725 | 1259 | 1454 | 2598 | 2992 |
| | ab initio | 2182i | 711 | 1260 | 1364 | 2577 | 2898 |
| $T_{s3}$ | PES | 1824i | 589 | 652 | 1351 | 1861 | 3039 |
| | ab initio | 1840i | 744 | 833 | 1246 | 1835 | 3127 |

[a] CCSD(T)/aug-cc-PVTZ. See figure 1 for the geometries corresponding to these stationary points.

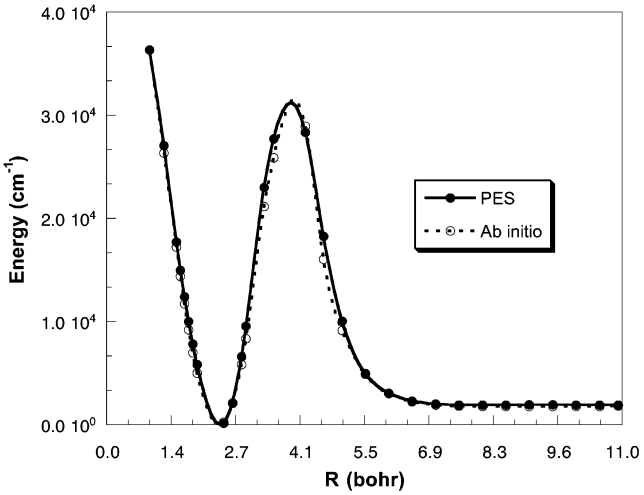


**Figure 3.** The potential energy as a function of $R$, where the molecule is fixed in a plane, and the $R_{CO}$, $R_{HH}$, and the angle between CO and HH bonds are optimized at each fixed $R$. The dashed line is the corresponding ab initio values.

$R_{MHa} < 10.0$, $3.0 < R_{MHb} < 50.0$, $0 < \alpha_a, \alpha_b < 180$, and $0 < \beta < 360$. From these symmetry unique points, permutation of the two hydrogen atoms generates a list of ~92 000 points which were fit in the manner descibed below.

Fitting the MR−CI points required three separate fits, denoted as fit a, fit b, and fit c, each on a different subset of the ~92 000 calculated points. All three subsets include only points in which $S_a < S_b$. Fit a is on ~27 000 points in the range $1.5 < S < 3.0$, fit b on ~33 000 points in the range $S > 2.0$, and fit c on 15 000 points in the range $S > 3.0$. The Morse expansion for fit a includes the same 896 terms (third order in the CO bond length and sixth order in all other coordinates) described in the previous section and resulted in an RMS deviation of 350 $cm^{-1}$. Fit b included 505 terms (same as fit a except those terms coupling the conserved modes, $R_{CO}$, $R_{CHa}$, and $R_{OHa}$, and the transitional modes, $R_{CHb}$, $R_{OHb}$, and $R_{HaHb}$, were restricted to fifth order) and resulted in an RMS deviation of 245 $cm^{-1}$. Fit c included 129 terms (same as fit c except terms involving only transitional modes were restricted to fifth order and terms coupling transitional and conserved modes were restricted to first order) and resulted in an RMS deviation of 175 $cm^{-1}$.

The three MR−CI fits were connected by the same style switching function as defined in subsection B. The switching coordinate $S$ is the same as that defined in subsection B for switching between the CCSD(T) and MR−CI fits. $S_{min}$ and $S_{max}$ for switching from fit a to fit b were set at 2.0 and 3.0, respectively, and 3.0 and 4.0 for switching from fit b to fit c. Finally, the MR−CI fit treats the two hydrogen atoms inequivalently, because of the point selection criterion $S_a < S_b$. This was required to get a good fit in the region near the H+HCO

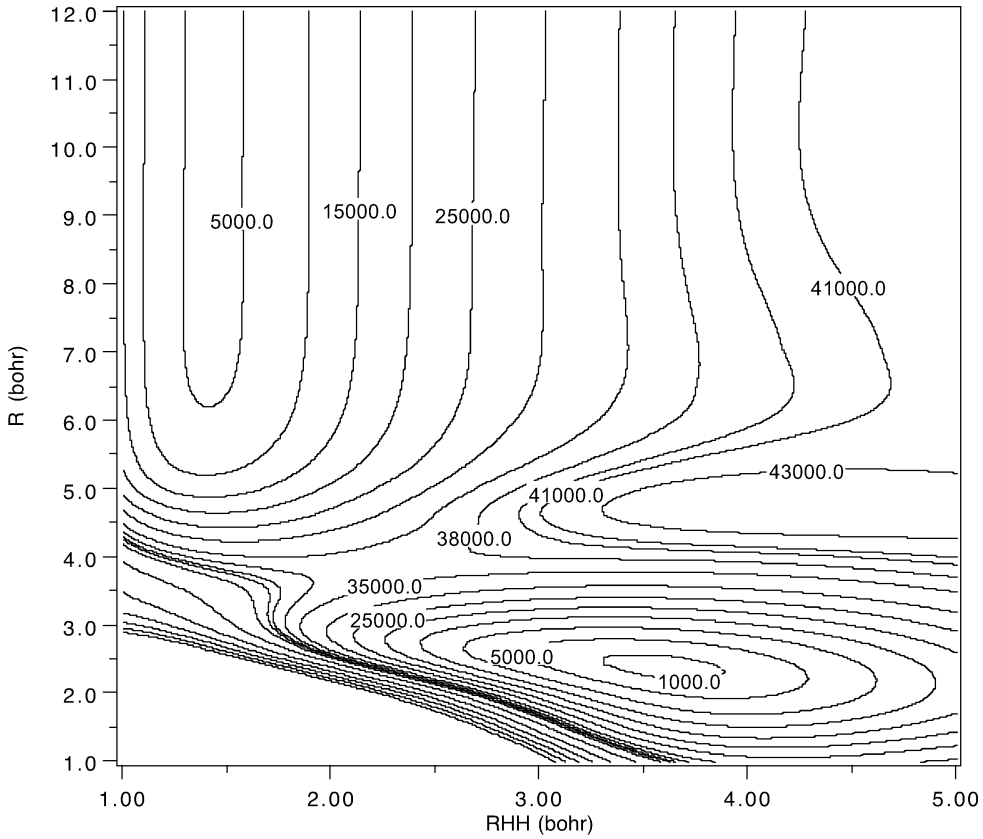


**Figure 4.** A contour plot of the PES ($cm^{-1}$) as a function of $R$ and $R_{HH}$, where the other variables are fixed at the global minimum.

asymptote. To enforce symmetry in the final fit, we simply reorder the two hydrogen atoms (if necessary) such that the criterion $S_a < S_b$ is satisfied.

## III. Results and Discussions

**A. Physical Properties of Stationary Points for the Fit.** A comparison of the geometries and energies of the $C_{2v}$ global minimum, the two isomers, *trans*-HCOH and *cis*-HCOH, and the saddle points denoted $TS_1$ (separating *trans*-HCOH and *cis*-HCOH), $TS_2$ (separating *trans*-HCOH and the global minimum), and $TS_3$ (separating the global minimum and the molecular products $H_2$+CO) from the fit and directly from the ab initio [CCSD(T)] calculations is given in Figures 1 and 2. The energies are relative to the global minimum. As seen, with the exception of the geometry and energy of $TS_1$, the values at the other stationary points of the fit agree very well with those from ab initio calculations. The error in the fit for this TS is not due to the switching function, because $TS_1$ is contained fully within the CCSD(T) part of the PES. Even for $TS_1$, the relative error of the fitted energy is only 3.23%, which is acceptable for dynamics studies. (It is perhaps worth noting that "direct-dynamics" calculations for the molecular and radical channels at this level of ab initio theory are not feasible.)

We carried out a normal-mode analysis at these six stationary points. The frequencies on the fitted potential are given in Table 2 and compared with those from ab initio calculations. The level of accuracy of results from the fit is acceptable for dynamics calculations, however, not for ones that demand "spectroscopic accuracy". We have done local fits around each stationary point and these produce highly accurate geometries, energies, and harmonic frequencies. These could be used in calculations that can be restricted to limited regions of configuration space. In addition, we are considering techniques to combine this set of local fits to obtain a smooth global one that would be an improvement over the one we present here.

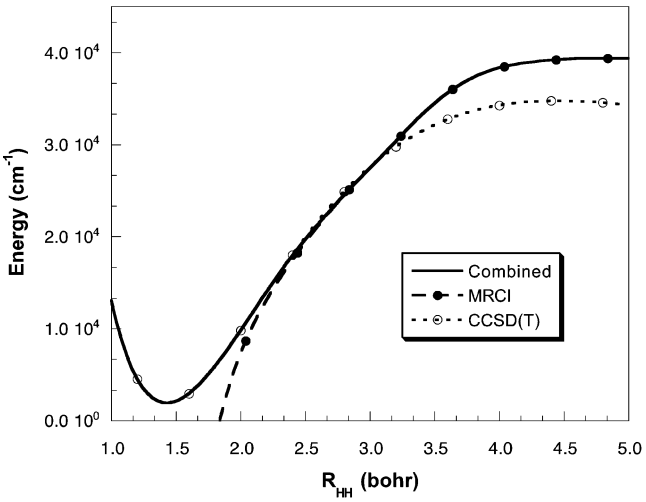


**Figure 5.** One-dimensional cuts as a function of $R_{HH}$, where the molecular are fixed in a plane, CO at equilibrium, and $R$ at 10 bohr.

**B. Molecular Channel $H_2CO \rightarrow H_2$+CO.** The barrier for the $H_2CO \rightarrow H_2$+CO reaction has been the focus of many ab initio calculations[14−16]. The barrier height for the molecular channel from the present PES is 30 583 $cm^{-1}$, which is 323 $cm^{-1}$ greater than the ab initio one (see Figure 2), but is quite close (fortuitously) to the best ab initio result of 30 683 $cm^{-1}$ reported by Feller et al.[16]

We investigated the molecular dissociation in more detail on the PES by means of a minimum energy path analysis. In this analysis, the four atoms are kept coplanar, and $R_{CO}$, $R_{HH}$, and the angle between the CO and HH bonds were optimized and the energy determined by doing additional ab initio calculations

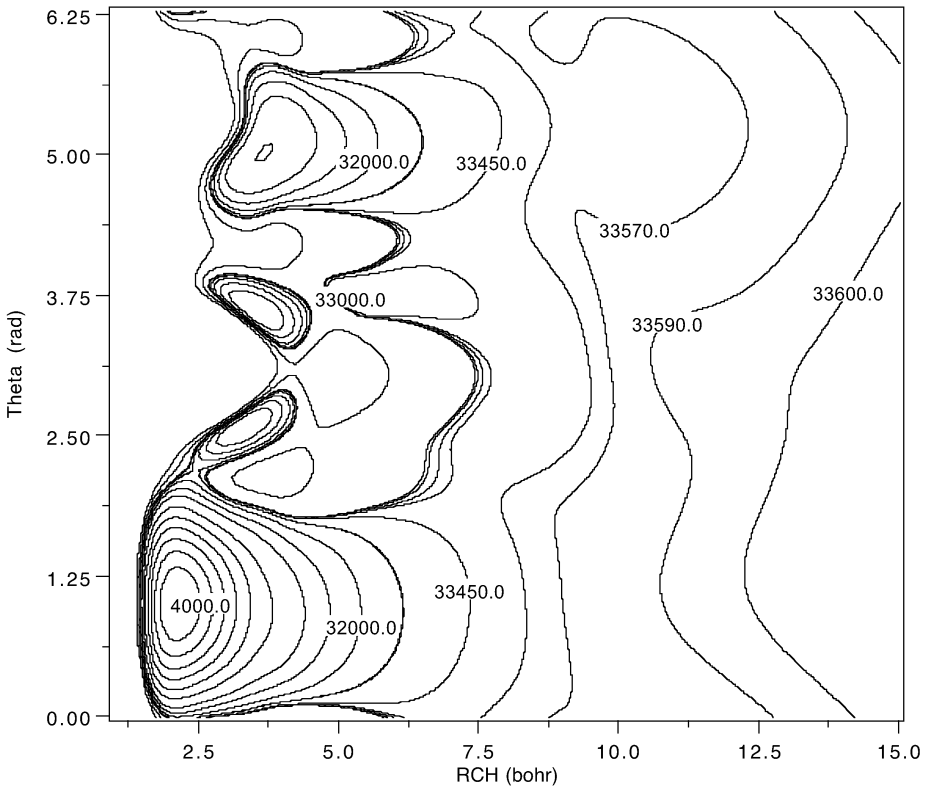


**Figure 6.** A contour plot of PES ($cm^{-1}$) as a function of $R_{CH}$ and theta, where theta is the angle between CO and CH bonds, and the other variables are fixed at the global minimum.

and using the PES, as a function of $R$, over the range 1.0−11. The results, shown in Figure 3, indicate that the PES gives a faithful and smooth representation of the ab initio calculations. The dissociation energy ($D_e$) from the PES is 1931 $cm^{-1}$, which agrees well with the best calculated value of 2028 $cm^{-1}$.[16] Thus, the present PES appears to give a good description of the dissociation behavior for the molecular channel.

A more global picture of the PES is shown in a contour plot as a function of $R$ and $R_{HH}$ in Figure 4, where the other variables are fixed at the global minimum. The molecular channel can be clearly seen with decreasing $R_{HH}$ and increasing $R$. The plot also illustrates that the switchings among the three CCSD(T) fits and between the CCSD(T) and MR−CI fits are quite smooth. Furthermore, Figure 4 shows that the global PES is well behaved in the high-energy break-up region H + H + CO. To examine the behavior of the switching in more detail, we plot the potential as a function of $R_{HH}$ for $R = 10$ in Figure 5. The plot shows the result from the CCSD(T)-based, MR−CI-based, and combined fits. As seen, the switch between the two former fits (which occurs in the range $2.175 \leq R_{HH} \leq 2.9$) yields a very smooth result and one that has the correct behavior in the break-up region H + H + CO.

**C. Radical Channels $H_2CO \rightarrow H+HCO$ and $H+HCO \rightarrow H_2+CO$.** Now consider the behavior of the PES for the radical channel and the region of the two isomers. Figure 6 shows a contour plot of the PES as a function of $R_{CH}$ and $\theta$, where $\theta$ is the angle between the CO and CH bonds, and the other variables are fixed at the global minimum. The range of $\theta$ describing a least-motion path for $H_2CO \rightarrow H+HCO$ is $0 < \theta < 1.9$. The regions of *trans*-HCOH and *cis*-HCOH are $2.0 < \theta < 3.1$ and $3.1 < \theta < 4.1$, respectively. The direct abstraction reaction $H+HCO \rightarrow H_2+CO$ is described by the region $4.3 < \theta < 6.0$. When $R_{CH}$ is large enough so that the H and HCO are noninteracting, the potential energy should be independent of $\theta$. As seen in Figure 6, for $R_{CH} > 12.0$, there is a small (roughly 10 $cm^{-1}$) "wiggle" in the PES, which should not introduce serious errors in dynamical studies.

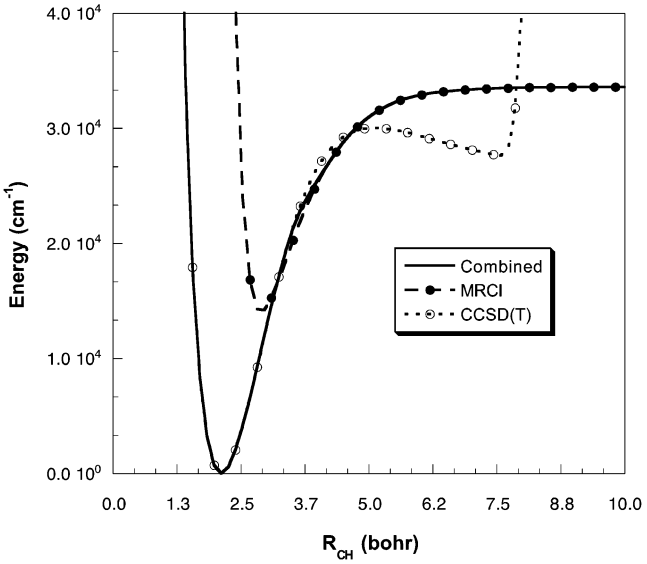


**Figure 7.** A cut as a function of $R_{CH}$, where the other variables are fixed at the global minimum.

From this figure, we also see that at about $\theta = 1.01$ $H_2CO$ dissociates to HCO+H without a barrier, as $R_{CH}$ increases. The dissociation energy, $D_e$, on the PES is 33 239 $cm^{-1}$ (see Figure 2). We calculated an approximate, harmonic zero-point correction using CCSD(T)/aug-cc-PVTZ calculations for the $H_2CO \rightarrow H+HCO$ of −2989 $cm^{-1}$ and obtain an approximate $D_0$ of 30 250 $cm^{-1}$ which compares very well with the experimental estimates of 30 278 $cm^{-1}$ [6] or 30 328 $cm^{-1}$.[7]

In the region of the switching between the CCSD(T)-based and MR−CI-based fits, the PES is also quite smooth. This is examined in more detail in Figure 7, where a cut through the

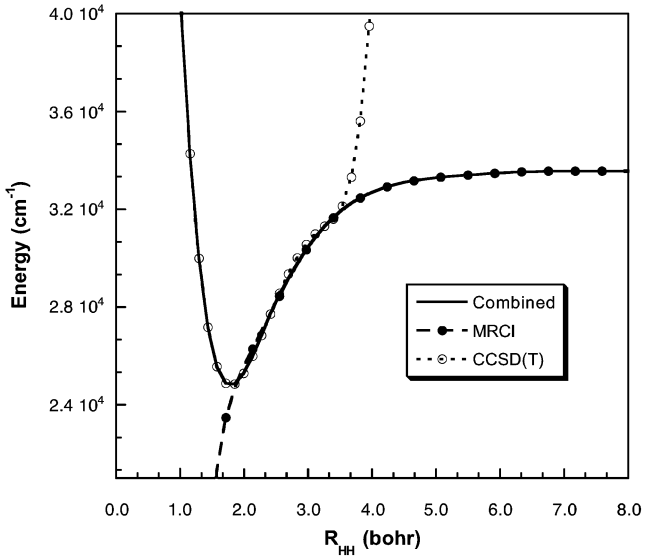


**Figure 8.** A cut as a function of $R_{HH}$, where the C and two H atoms are set in line, and the other variables are fixed at the global minimum.

PES describing the $H_2CO \rightarrow H+HCO$ channel is shown as function of $R_{CH}$ where the value of the three HCO internal coordinates are held fixed at their values at the $H_2CO$ global minimum. As seen, there is a smooth transition from one fit to the other.

In Figure 8, we show another cut as a function of $R_{HH}$, where now the C and two H atoms are collinear, and the other variables are fixed at the global minimum. From this figure, we see that there is no barrier for the abstraction reaction $H+HCO \rightarrow H_2+CO$ on the PES. This reaction has been postulated[9] as a second mechanism for molecular elimination, one that does not involve $TS_3$. The good representation of both this abstraction reaction and $TS_3$ on the combined PES now makes it possible to test this hypothesis in future studies of the $H_2CO$ dissociation dynamics.

## IV. Summary

A global potential energy surface for $H_2CO$, describing the molecular and radical dissociation channels and cis and trans HOCH isomers, has been constructed by fitting tens of thousands of CCSD(T)/aug-cc-PVTZ and MR−CI/aug-cc-PVTZ calculations of electronic energies. The PES is obtained from three local CCSD(T)-based fits and three MR−CI fits, connected smoothly by five switching functions. The RMS error of one extensive fit, describing the $H_2CO$ minimum, the two isomers, and the molecular dissociation saddle point is 648 $cm^{-1}$ for energies up to 38 500 and a data set of 31 336 energies.

The geometries, energies, and harmonic frequencies of the six stationary points are calculated on the new PES and the agreement with the ab initio results is good. Analyzing one-dimensional cuts along selected coordinates and contour plots shows that the molecular and radical channels are represented well by the new global PES. Furthermore, the PES can also describe the high-energy reaction $H_2+CO \rightarrow H+H+CO$ and the abstraction reaction $H+HCO \rightarrow H_2+CO$. Calculations of the abstraction reaction are underway.

Finally, this surface is available upon request.

**Acknowledgment.** This work was supported by the U.S. Department of Energy, Office of Basic Energy Sciences, Division of Chemical Sciences, Geosciences and Biosciences, under Contract W-31-109-ENG-38 (Argonne) and grant DE-FG02-97ER14782 (Emory).

## References and Notes

(1) Houston, P. L.; Moore, C. B. *J. Chem. Phys.* **1976**, *65*, 757.
(2) Yeung, E. S.; Moore, C. B. *J. Chem. Phys.* **1973**, *58*, 3988.
(3) Moore, C. B.; Weisshaar, J. C. *Annu. Rev. Phys. Chem.* **1983**, *34*, 525.
(4) Butenhoff, T. J.; Carteton, K. L.; Moore, C. B. *J. Chem. Phys.* **1990**, *92*, 377.
(5) Polik, W. F.; Guyer, D. R.; Moore, C. B. *J. Chem. Phys.* **1990**, *92*, 3453.
(6) Terentis, A. C.; Kable, S. H. *Chem. Phys. Lett.* **1996**, *258*, 626.
(7) Chuang, M.; Foltz, M. F.; Moore, C. B. *J. Chem. Phys.* **1987**, *87*, 3855.
(8) Valachovic, L. R.; Tuchler, M. F.; Dulligan, M.; Droz-George, Th.; Zyrianov, M.; Kolessov, A.; Reisler, H.; Wittig, C. *J. Chem. Phys.* **2000**, *112*, 2752.
(9) Zee, R. D.; Foltz, M. F.; Moore, C. B. *J. Chem. Phys.* **1993**, *99*, 1664.
(10) Jalbout, A. F.; Chang, C. M. *Theo. Chem*. **2003**, *634*, 127.
(11) Deng, L.; Ziegler, T.; Fan, L. *J. Chem. Phys.* **1993**, *99*, 3823.
(12) Jensen, F. *Theo. Chem. Acc.* **1998**, *99*, 295.
(13) Bauerfeldt, G. F.; Albuquerque, L. M. M.; Arbilla, G.; Silva, E. C. *Theo. Chem.* **2002**, *580*, 147.
(14) Dallos, M.; Lischka, H.; Monte, E. V.; Hirsch, M.; Quapp, W. *J. Comput. Chem.* **2001**, *23*, 576.
(15) Yamaguchi, Y.; Wesolowski, S. S.; Huis, T. J. V.; Shaefer, H. F. *J. Chem. Phys.* **1998**, *108*, 5281.
(16) Feller, D.; Dupuis, M.; Garrett, B. C. *J. Chem. Phys.* **2000**, *113*, 218.
(17) Li, X.; Millam, J. M.; Schlegel, H. B. *J. Chem. Phys.* **2000**, *113*, 10062.
(18) Chen, W.; Hase, W. L.; Schlegel, H. B. *Chem. Phys. Lett*. **1994**, *228*, 436.
(19) Carter, S.; Mills, I. M.; Murrell, J. N. *Mol. Phys.* **1980**, *39*, 455.
(20) Farantos, S. C.; Murrell, J. N. *Mol. Phys.* **1980**, *40*, 883.
(21) Yonehara, T.; Kato, S. *J. Chem. Phys.* **2002**, *117*, 11131.
(22) Chang, Y.; Minichino, C.; Miller, W. H. *J. Chem. Phys.* **1992**, *96*, 4341.
(23) Handy, N. C.; Carter, S. *Chem. Phys. Lett*. **1981**, *78*, 118.
(24) Thompsons, K. C.; Jordan, M. J. T.; Collins, M. A. *J. Chem. Phys.* **1998**, *108*, 8302.
(25) MOLPRO is a package of ab initio programs written by Werner, H.-J.; Knowles, P. J. with contributions from Almlof, J., Amos, R. D., Berning, A., Cooper, D. L., Deegan, M. J. O., Dobbyn, A. J., Eckert, F., Elbert, S. T., Hampel, C., Lindh, R., Lloyd, A. W., Meyer, W., Nicklass, A., Peterson, K., Pitzer, R., Stone, A. J., Taylor, P. R., Mura, M. E., Pulay, P., Schutz, M., Stoll, H., Thorsteinsson, T.
(26) Dunning, T. H., Jr. *J. Chem. Phys.* **1989**, *90*, 1007.
(27) Kendall, R. A.; Dunning, T. H., Jr.; Harrison, R. J. *J. Chem. Phys.* **1992**, *96*, 6796.
(28) Woon, D. E.; Dunning, T. H., Jr. *J. Chem. Phys*. **1993**, *98*, 1358.
(29) Hampel, C.; Peterson, K.; Werner, H.-J. *Chem. Phys. Lett*. **1992**, *190*, 1
(30) Werner, H.-J.; Knowles, P. J. *J. Chem. Phys*. **1988**, *89*, 5803.
(31) Knowles, P. J.; Werner, H.-J. *Chem. Phys. Lett*. **1988**, *145*, 514.
(32) Zou, S.; Bowman, J. M. *Chem. Phys. Lett*. **2003**, *368*, 421.